NUMERICAL SIMULATION OF THE CATASTROPHIC EARTHQUAKE AND TSUNAMI IN CHILE ON 9 MAY 1877

Mazova R.Kh [1,2], Baranova N.A [3], Alekseev D.A.[1,4,5], Lobkovsky L.I.[1,4]
J. F.[6], Oses G. A.[6], Jorge Van Den Bosch F.[6], Gustavo Oses A.[6]

[1]*P.P. Shirshov Institute of Oceanology RAS, Moscow 917435 Russia,*
e-mail address: llobkovsky@ocean.ru
[2]*R.E. Alekseev Nizhny Novgorod State Technical University, 24, Minin str., 603095*
Nizhny Novgorod, Russia. e-mail address: raissamazova@yandex.ru
[3]*uriga, 6/6 Nartova st., office 829, 603104 Nizhny Novgorod, Russia.*
e-mail address: Natalia.baranova@inbox.ru
[4]*Moscow Institute of Physics and Technology (MIPT), Moscow Region, Russia*
[5]*Schmidt Institute of Physics of the Earth RAS, Moscow 917435 Russia,*
alexeevgeo@gmail.com
[6]*Engineering Center Mitigation Natural Catastrophes Faculty of Engineering,*
University of Antofagasta, Antofagasta, Chile. e-mail address:
Jorge.VanDenBosch@uantof.cl   Gustavo.oses@uantof.cl

ABSTRACT

In this paper, on the basis of the available historical data and geodynamic studies, numerical simulation of the historical catastrophic earthquake and tsunami of May 9, 1877 is carried out by making use the so called "keyboard" geodynamical model providing the computational formalism for seismic cycles and crustal block motion analysis. 23 scenarios of the kinematic movement of the keyboard blocks were implemented, when the earthquake source was fragmented from larger to smaller segments. Using the proposed methodology, for each scenario, the generation of a tsunami source is simulated and the computation of wave fields up to the 5-meter isobath is carried out. Analysis of the entire set of simulated earthquake scenarios makes it possible to choose a tsunamigenic earthquake scenario with the most adequate characteristics of tsunami waves in the coastal zone. The results obtained are compared with both historical data and those obtained for this event by other authors using various numerical models. Large-magnitude earthquakes in northern Chile and

southern Peru occur every 108 years on average. It should be noted that over 143 years since the catastrophic earthquake of May 9, 1877, any similar events were completely absent. In 2007, a 7.7 Mw earthquake occurred near Tocopilla, and in 2014 a catastrophic $M = 8.1$ earthquake hits Pisagua. It is believed that only part of the energy accumulated over 143 years has been released during those events, while most of it is yet to be released. Thus, we can conclude that a serious tsunami hazard exists for all coastal cities of southern Peru and northern Chile.

Key words: *earthquake source, tsunami source, numerical simulation of tsunami.*

1. INTRODUCTION

At approximately 8:30 pm on Wednesday, May 9, 1877, a strong $M = 8.7$ earthquake struck near Patache (González-Corrasco et al., 2020), with shakes being strongly felt in La Paz, Bolivia, about 550 km away from the epicenter area. It also caused pronounced tremors in Santiago de Chile, at a distance of 1400 km from the source (Vidal Gormáz, 1884), and resulted in extensive rupturing from the north of Pisagua to Mejillones region, (González-Corrasco et al., 2020), see Fig.1 where the blue ellipse shows the size of the rupture zone during the 1877 earthquake. Historical notice describing this great earthquake and tsunami, was written by Francisco Vidal Gormáz in November 1877, and published later in 1884 from which we have extracted important data.
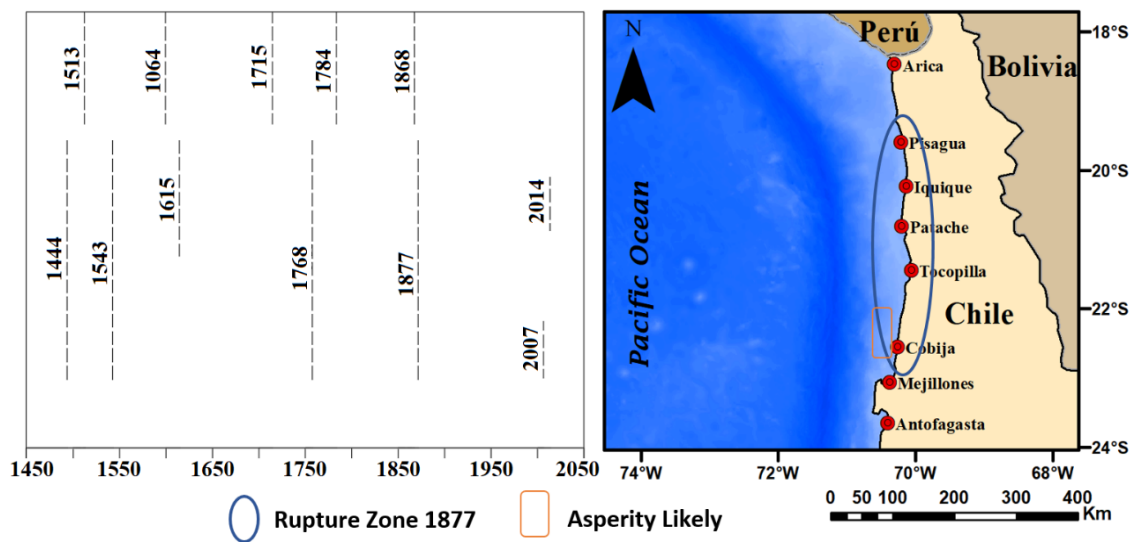

Fig. 1. Great earthquake and tsunami sequence in the northern Chile and southern Peru. taken from (Vargas et al., 2005) and modified in the right panel to include the names and locations of the historical and current cities. The ellipse corresponds to the rupture zone.

The coastal areas of northern Chile and southern Peru are the ones of the most active in the world in terms of seismicity, with frequent occurrence of large-magnitude earthquakes, both in the present and in the recent past due to the proximity of the subduction interface between Nazca and South American tectonic plates, extending from Colombia to the Taitao Peninsula in the extreme south of Chile (CIGIDEN, 2017). In this region, the historical and paleo-historical evidence indicates a series of great earthquakes accompanied by transoceanic tsunamis that show the potential for the similar events in the near future. This series begins in 1444 (this year it was based on a study of drilling of the seabed in the bay of Mejillones (Vargas et al., 2005)), followed by historical large-magnitude earthquakes in 1543, 1615, 1768, and 1877 (Fig. 1; Vargas et al., 2005), with average time interval between great earthquakes being 108 years.

The direct observation shows the absence of a large-magnitude earthquake after 1877 (Fig. 1) during the 143 years following the event. In 2007, a $M = 7.7$ earthquake occurred near Tocopilla, and in 2014 there was another one $M = 8.1$ shock near Pisagua and Iquique, however it is believed that those events led to partial release of the accumulated energy, while most of the stress remains to be released in the future (Chlieh et al., 2011; González-Corrasco et al. to 2020). The seismic rupture in southern Peru and northern Chile is believed to likely cause in the nearest future an earthquake with magnitude of up to 8.9 (see, e.g. (Mazova & Ramirez, 1999)). Thus, we can conclude that a serious tsunami hazard exists for all coastal cities in southern Peru and northern Chile. The nature of the generated tsunami waves, for each of catastrophic events of the Chilean coast, their distribution and behavior in the coastal zone, have been analyzed in sufficient detail in the literature (see, e.g., Pararas-Carayannis 2010; Okal et al., 2006; Kulikov, 2005; Vargas et al., 2005; Mazova and Ramirez 1999; Ramirez et al. 1997; Mazova and Soloviev1994).

Therefore, it is likely that in the near future this series will be continued with much stronger earthquake, accompanied by a devastating tsunami. Obviously, simulating such an event employing the modernized computational methods will allow for the development of an adequate response to protect the communities at risk, both in northern Chile and probably in the rest of the Pacific Ring of Fire. At the same time, knowledge of the history of this event is of great importance when choosing seismic modeling scenarios that are closest to historical data, so that the modeling results could reliably simulate the possible aftermath.

From the analysis of the tsunami wave arrival times at three nearby locations, available from the historical records, it can be seen that the first wave arrived at Cobija 7 minutes after the earthquake, at Mejillones 20 minutes after the shock and at Antofagasta 15 minutes post earthquake. At Iquique, the wave came about half an hour later, since the historical evidence indicates that immediately after the quake, the firefighters were scooping water from the sea to extinguish the fires caused by the earthquake in the coastal area of the city before tsunami (Vidal Gormáz, 1884). There is no specific arrival time available for Arica, which suggests that it took the wave about half an hour to reach this location. From the above it can be concluded that the maximum seafloor displacement, triggering the tsunami, most likely occurred between the northernmost Mejillones and Cobija, consequently it can be assumed that there was an important asperity, in the Fig. 1 the red rectangle corresponds to size of the asperity likely probable, estimated from the

arrival times of the first tsunami waves recorded in history at Cobija 7 min, Mejillones 20 min and Antofagasta 15 (Vidal Gormáz, 1884).

Similarly, during the Antofagasta $M = 8.1$ earthquake in July 1995, by making use of the first tsunami wave arrival times at three tide gauges it was possible to determine the tsunami's source location, 100 km south of the epicenter, near Caleta Blanco place (Ramírez et al., 1997). In a later study, the Nazca plate dislocation contour map was compiled (Mendoza, 1997), showing the maximum displacement (2 meters in magnitude) in this particular area, while in the epicentral region the dislocation is smaller, around 1 m (Fig. 2). There, in the maximum dislocation area, the coseismic acceleration must have been higher than the one recorded in the city of Antofagasta (275 см / c^2, UCN 1995), where despite the proximity to the epicenter (22 km) there were only minor damages. No doubt, if the city of Antofagasta had been located 80 km further south, the earthquake would likely devastate it.
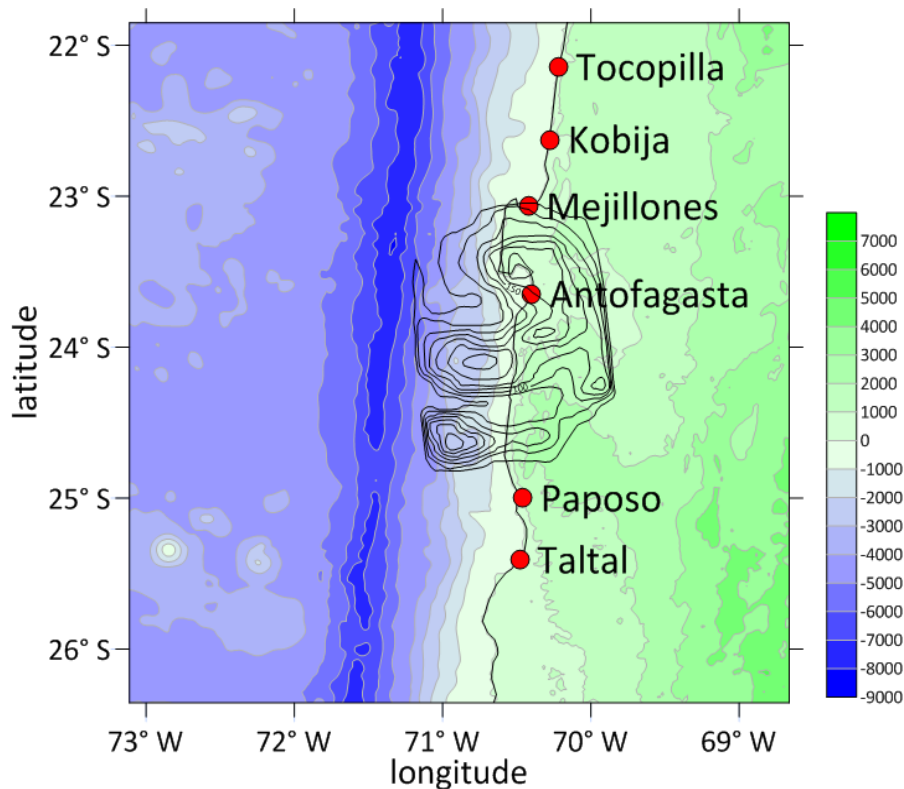

Fig. 2. Large-magnitude block displacement seen from Nazca plate surface contour map created for 1995 Antofagasta earthquake (for more details, see (Mendoza, 1997)).

According to the model presented in (Kanamori & Stewart, 1978; Lay & Kanamori, 1981), such regions with the highest energy release are called asperities. Transoceanic tsunami caused by 1877 earthquake was recorded at multiple locations around globe, with heights of about 1.5 m in New Zealand, 3 m with severe damage in Hawaii and Makai Island, 4 m with severe damage at Marquesas Islands. In Acapulco, Mexico, the flood

reached the central square (Vidal Gormáz, 1884). The highest flood levels causing severe damage and numerous human fatalities were observed in northern Chile and southern Peru (north to south): 19 m in Arica, 9 m in Iquique (estimated from historical data in (Titichoca and Guiñez, 1992)), 11.9 m in Cobija, 11.5 m in Mejillones, 6 m in Antofagasta. In Chañaral city located 300 km south of Antofagasta, tsunami had caused severe damage, but the data on flood levels weren't available, as the town has changed its location several times. Starting from 26º south latitude southwards, the flood levels began to decrease. Another interesting evidence says that a 27-meter-high seafloor rise occurred in the Pisagua port area, accompanied by a 2-meter wave run up (Vidal Gormáz, 1884), which is also an important constraint for justification of the geodynamical model employed for tsunami simulation.

2. DESCRIPTION OF EARTHQUAKE NEAR NORTH-WESTERN CHILEAN COAST ON 9 MAY1877

On May 9, 1877, at 21:16 local time, an earthquake and subsequent tsunami were recorded in the area of the city of Iquique. The epicenter of the earthquake was in the Pacific Ocean near the city of Iquique. The greatest intensity was noted between the cities of Arica, Iquique and Antofagasta, and Tocopilla, Gatiko and Cobija were also severely affected. All these cities were destroyed. Earthquake victims were recorded in the area from Pisco to Antofagasta. In Iquique, Gatiko and Cobija, five minutes after the earthquake, tsunami waves arrived with a slow rise in sea level, the wave height eventually ranged from 10 to 15 meters. The second wave was more powerful - its height was from 20 to 23 meters, and it came 15 minutes after the main shock, and this wave destroyed the buildings that remained standing after the earthquake.

In Mejillones, an earthquake of exceptional strength lasted 7 minutes, and the second wave was reported to be 23 meters high. In Iquique, 20 minutes before the earthquake, a faint rolling rumble was heard, accompanied by slow vibrations of the earth, which soon turned into terrible tremors that lasted about 4 minutes. The first wave came 20-30 minutes after the earthquake and was not high. But the second wave was much more intense.

In Antofagasta, the tremors were very strong, the houses swayed like ships during a storm. During the earthquake, the ocean was completely calm, but 10 minutes after the earthquake it overflowed the coast - the tsunami devastated the coastal part of the city. The height of the flood, according to some estimates, was 6 m, according to others - 2.5 m above mean ocean level or 2 m above tide level.

A terrible rumble accompanied an earthquake in San Pedro. In Caleta-Pabellon de Pica, an earthquake with increasing strength lasted 5 minutes and about 25 minutes after the earthquake, the ocean hit the shore. In Chanabaya, the retreat of water was noticed immediately after the earthquake, out of 400 houses, allegedly, only two survived. In 20 minutes after the beginning of the tremors, the tide came. There were three waves at intervals of 8-10 minutes. The second wave was the largest and rose to a height of up to 10 m.

In Tocopilla, the ocean rose 15 min (according to other sources, 30 min) after the earthquake. The height of the rise is estimated at 24 m. Tocopilla was destroyed. In Caldera, the earthquake was of moderate intensity and lasted for about 3 minutes. At about 21 hours the ocean began to recede from the coast, and at about 21:30 the first high tide came. The highest heights are 2 m above the mean ocean level. It was stronger in Copiapo. In Coquimbo, the earthquake lasted 4-5 minutes. Valparaiso has a long but weak earthquake. In Punta Lobos, immediately after the earthquake, the ocean moved away from the coast and after 10 minutes it returned in the form of a tidal wave 6 m high. After 30 minutes, a second wave surged in, washing everything off to a height of 10 m.

Table 1. Impact of Tsunami on Coastal Cities (Soloviev and Go, 1975)

Observation point	Time between earth-quake and the beginning of noticeable level of oscillations (hours)	Maximum wave height (м)	Manifestations and the sequence of the tsunami
Arica	0.7	8-9	The lower part of the city was washed away
Pisagua	2.5	5	The train station and other buildings were destroyed
Iquique	0.3	6	The lower quarter of the city, the customs, were washed away; brought ashore, sunk or damaged ships and boats; killed 30 people
Chanabaya	0.1	10	The city is completely flooded; victims; ships were killed
Caleta Pabellon de Pica	0.4	10	The lower part of the city is destroyed; sunk 5 ships and 27 homes damaged
Punta-Lobos	0.1	10	2 ships sunk and 14 damaged
Huanillos	0.25	9-18	20 houses were washed away; 4 ships sunk and 13 damaged; victims
Tocopilla	0.1	24?	Houses were destroyed and washed away
Cobija	0.1	9	¾ cities were flooded 14 people were killed.
Mejillones	0.5	21	2/3 of the city destroyed; 33 people were killed
Antofagasta	0.1	6	Homes w3as destroyed
Chanyaral	0.9	4-5	City partially flooded
Caldera	0.7	2	-
Carrizal-Bajo	2	1.5	The ships suffered
Coquimbo	2	2	-
Valpariso	2.5	1.1	-
Costitucion	1.5	3	-
Tome	3.5	0.7	-

The complexity of the numerical simulation of this earthquake is associated with a significant discrepancy between field data in some of the considered settlements, given in different sources. Below are data on wave heights from several sources (Soloviev and Go, 1975; Diaz, 1992; Araneda et.al, 2003; Okada, 1992; Barrientos and Ward, 2009; Gusiakov, 2021; Tsunamis in Peru-Chile (noaa.gov); NGDC/WDS Global Historical Tsunami Database (https://www.ngdc.noaa.gov/hazard/ tsu_db.html) (see. Table 2).

Table 2. Refined data on the heights of the tsunami wave run-up during the 1877 earthquake (Soloviev and Go, 1975; Diaz, 1992; Okada, 1992; Barrientos and Ward, 2009).

№	Point	Runup height (m) (Soloviev and Go, 1975	Runup height (m) (Okada, 1992, Barrientos and Ward, 2009)
1	Arica	9	20
2	Pisagua	5	-
3	Iquique	6	9
4	Chanabaya	10	-
5	Caleta Pabellon de Pica	10	-
6	Punta-Lobos	10	-
7	Huanillos	14	-
8	Tocopilla	24	-
9	Cobija	9	12
10	Mejillones	21	12
11	Antofagasta	6	7

1. STATEMENT OF THE PROBLEM

It is well known that the nature of a tsunami depends on the dynamics of displacements in the zone of the earthquake source. Localization of earthquake source for 1877 event, taken from documental data (Gebco Digital Atlas), is presented in Fig.3. (a). In most cases, wave generation computations use seismic data to determine source displacement. Then the static problem of recalculating the displacements of the bottom to the ocean surface is solved. Depending on the speed of movement of the blocks in the seismic source, various scenarios for the formation of a tsunami source on the water surface can be realized. This 1877 event of earthquake and tsunami was studied in many works (see, e.g. Silgado, 1985),). In work (Barrientos and Ward, 2009), the tide gauge data of the 1877 tsunami and the recent tsunami data from strong earthquakes were compared, and numerical simulations were performed.

The parameters of the seismic source were consistent with the works (Abe, 1972; Diaz, 1992), where, based on the characteristics of the run-up and the time of arrival of waves at the coast, the maximum rupture length was estimated at 500 km and the corresponding displacement of 10 m for the 1877 event. In work (Riquelme et al., 2012), where the study of the 1877 event was also carried out, it was noted that the parameters of the fault and the slip distribution of this earthquake are not well studied, because only a few tide gauges recorded this event at a great distance
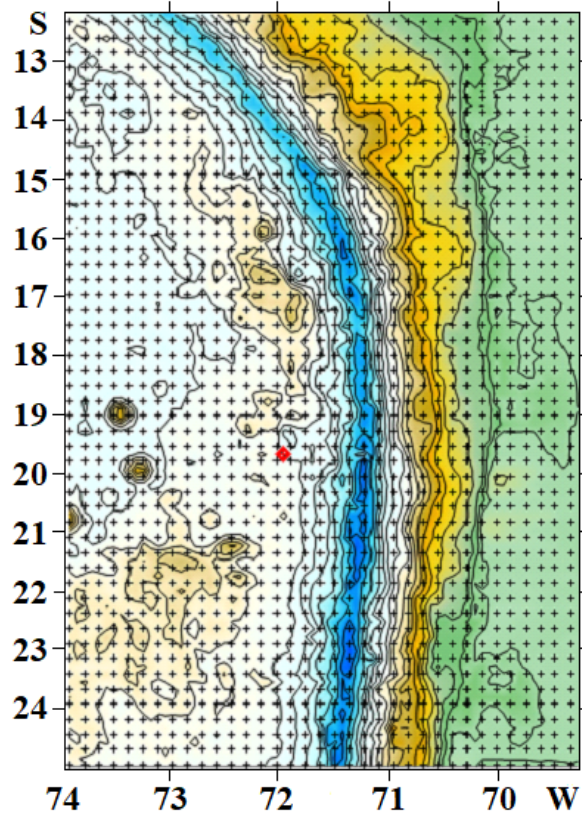

Fig. 3. Bathymetric (a) and geographical (b) maps of the northwestern part of the Chilean coast. The red dot indicates the epicenter of the 1877 earthquake. (Gebco Digital Atlas)

Therefore, to numerically simulate the generation and propagation of tsunamis, they used several rupture scenarios using the NEOWAVE software package. The recent work (Ruiz and Madariaga, 2018), had demonstrated that "subduction earthquakes present a large diversity that it is not incorporated in the traditional interpretation of Chilean seismicity".
In Fig. 4, the seismotectonic map of the northern Chile and southern Peru subduction zone is presented. In this figure, "dark red dots correspond to the subduction area. The information was processed by the GFZ with a change in the localization of about 300 epicenters in this area. The information was used as an earthquake subduction domain to simulate the process. The area in the green rectangle corresponds to the start area of the simulation. The red line corresponds to the total data set. Table 3 and Fig.5 show the data on the land deformation for the tsunami of 1877 and fault parameters (SHOA, 1997), which

were used by us for the initial assessment of the seismic source (see also (Ruiz et al., 2015)).
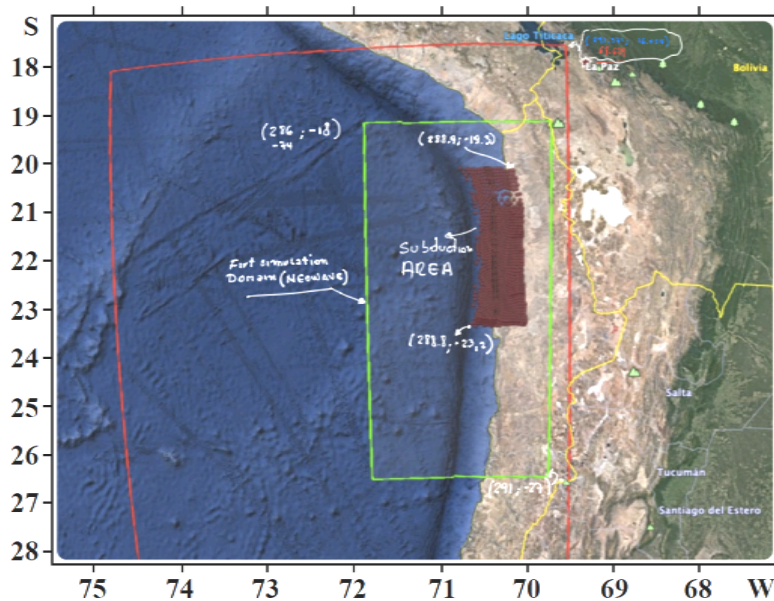

Fig. 4.. Map with marked subduction zone and computed area by Gabriel Álvarez A. (2019) "Centro Ingeniería Mitigación Catástrofes Naturales Facultad de ingeniería. Univ. Antofagasta. Chile.

Table 3: Land deformation generated by earthquake 1877.

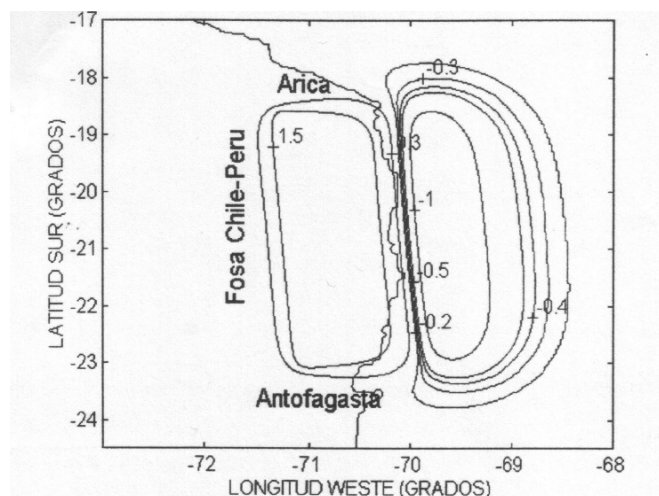| SOUTH END	Dislocation	Long	Width	Rhumb	DIP	DEPTH	Angle of Displacement
23° S 71° W	12 m.	490 Km.	150 Km.	359°	19°	10 Km.	90°

Fig. 5. Slab surface displacement generated by 1877 earthquake. Contour-line lables show dislocation in meters (SHOA, 1997).

The left panel in Fig. 6. shows the tsunami and paleotsunami database relative to the coastal zone. The localization of the source of the 1877 earthquake is marked in red. On the right panel, a part of the computation area used to computation the earthquake of 1877 by ("Centro Ingeniería Mitigación Catástrofes Naturales Facultad de ingeniería. Univ. Antofagasta. Chile."), as well as a section of the coastal zone with the marked localization of the seismic source are presented.
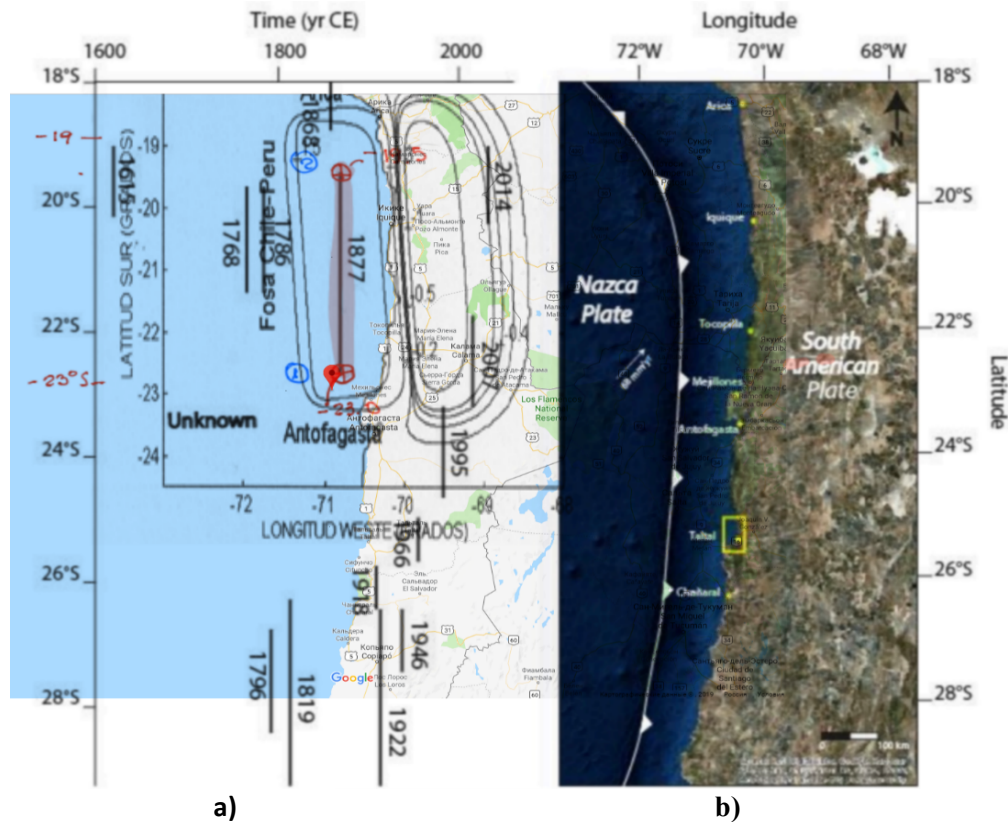

Fig. 6. a) Tsunami database for the earthquake coastal zone (for more details, see (DATA, 2021); b) as well as a section of the coastal zone with a marked localization of the seismic source (Barrientos and Ward, 2009; Comte and Pardo, 1991).

4. NUMERICAL SIMULATIONS OF THE 1877 TSUNAMI IN NORTHERN CHILE

Using the key-block model by Lobkovsky (Lobkovsky & Baranov, 1984) and the available geophysical and seismological data, the displacements of blocks in the earthquake source were preliminary estimated for the concrete scenarios. These estimates were used to obtain the tsunami source under using nonlinear shallow water equations (see, e.g., Voltzinger et.al, 1989; Pelinovsky, 1996; Lobkovsky et.al, 2006; Lobkovsky et.al, 2017; Mazova et.al, 2018) we obtain the formation of a tsunami source on the water surface above the earthquake source. Since the movement of the blocks occurs alternately at

different speeds and has a different displacement, the formation of the tsunami source and wave propagation from it is a continuous process from the moment the first block begins to move in the earthquake source.

The very formation of the tsunami source and the further propagation of waves in the near part of the coastal water area is a complex process determined by both the given scenario of block movement and the geometry of the coastal zone (see Fig. 3.). Wave propagation into the open ocean obviously has a simpler picture. The computation of this tsunami was carried out by various groups of scientists, according to different programs (see above), including the program (Okada, 1992). But such computations, on the information of Chilean group of co-authors did not give results close to real data. Using the data on the isoseims of the 1877 earthquake, the regions where the highest tsunami intensity was noted, the wave heights on the coast, taking into account the phase of the wave approach to the coast (Soloviev and Go, 1975), and the data on the heights at the same points given in (Diaz, 1992; Okada, 1992; Barrientos and Ward, 2009; Gusiakov, 2021; NGDC/WDS, 2021), a map of the computational area was compiled with points along the coast and the localization of the seismic source of the 1877 earthquake (Fig.7).
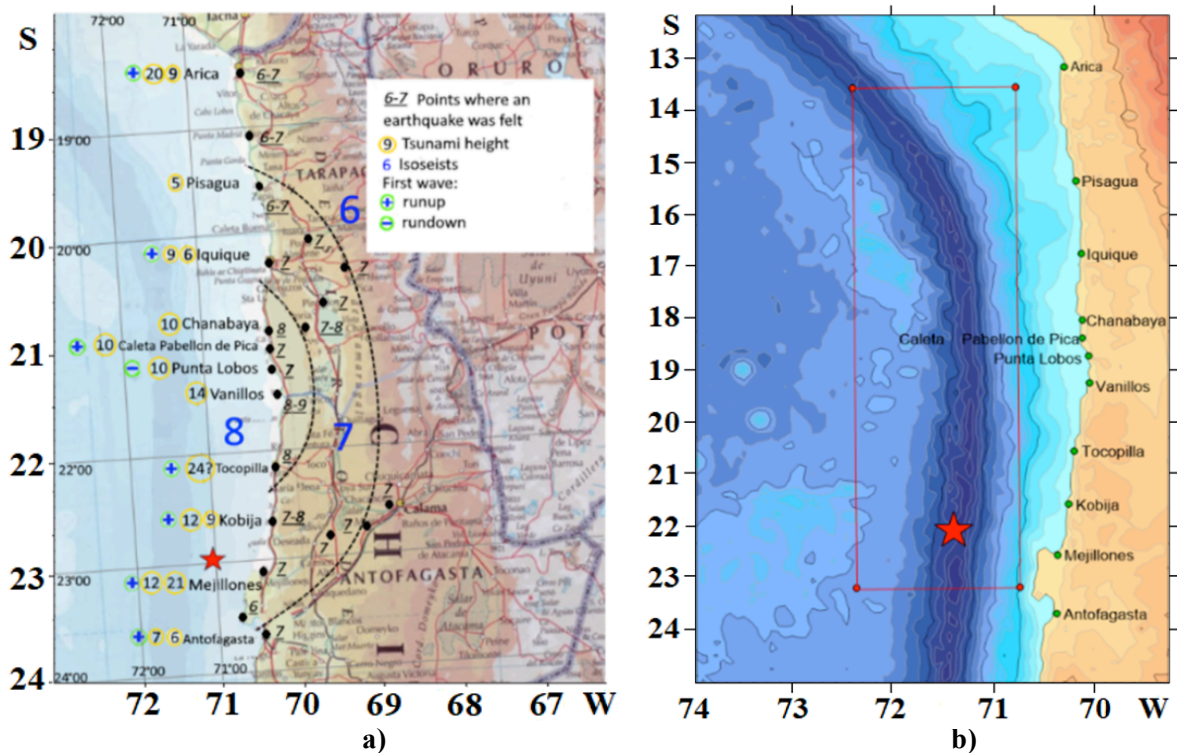

Fig. 7. a) Computational domain based on the data proposed in (Soloviev and Go, 1975; Diaz, 1992; Okada, 1992; Barrientos and Ward, 2009): large blue numbers identify the areas where the tsunami was most intense; small numbers - data on tsunami heights at a particular point based on data from works (Soloviev and Go, 1975; Diaz, 1992; Okada, 1992; Barrientos and Ward, 2009); signs (+) and (-) near the numbers on the left determine the nature of the approach of the first wave to the shore: (+) wave run-up to the shore, (-) wave rollback from the shore; dotted black lines - isoseismic; b) The initial contour of the earthquake source of 1877 (according to the initial data 530 x 150 km); The red asterisk is the epicenter of the earthquake.

It should be noted that the data on wave heights at coastal points (numbers in yellow circles) shown on this map in a number of points, differ significantly from each other, although they represent real data taken from works (Soloviev and Go, 1975; Diaz, 1992; Okada, 1992; Barrientos and Ward, 2009; Gusiakov, 2021; NGDC/WDS, 2021) which we had to determine when calculating. The same data are presented further in the Tables comparing the obtained computation results with field data.

In the course of the study, 23 Scenarios of various kinematic movements of the keyboard blocks were considered, into which the earthquake source was fragmentally split divided. The fragmentation of the earthquake source into sub-faults was determined both by documentary data on descriptions of earthquakes and tsunamis at specific points on the coast (Soloviev and Go, 1975; Diaz, 1992; Barrientos and Ward, 2009). Multi-block sources of a virtual earthquake with the given characteristics of the process were considered: 4-block, 8-block, 12-block, 13-block and 14-block, and the parameters of a possible tsunami were estimated at 11 points of the coast, for which there is documentary evidence in various literature. In this work, 4 computations with the closest data to the documentary ones are presented. Estimates of the tsunami arrival times at various locations along the coast for the events of 1877, given in (Soloviev and Go, 1975; Diaz, 1992), made it possible to determine the maximum rupture lengths in the source of more than 500 km. Based on the data of the works (Soloviev and Go, 1975; Diaz, 1992; Okada, 1992; Barrientos and Ward, 2009), which provide different data about earthquake magnitude, computations were carried out for $M = 8.5$ and $M = 8.8$.

Using the ratio of the earthquake magnitude and the characteristics of the rupture in the earthquake source (Diaz, 1992), using the formulas of (Wells and Coppersmith, 1994) and (Iida, 1963) we obtained the following estimates for the length and width of the rupture in the earthquake source.

$$\lg L = 0.59\, M\,\text{w} - 2.44 +/- 0.16,\ (L \text{ in km})$$

$$\lg W = 0.32\, M\,\text{w} - 1.01 +/- 0.15,\ (W \text{ in km}) \tag{1}$$

where L is the length of the rupture in the source, W is the width of the rupture plane:

For a magnitude $M = 8.5$ from formulas (1) we obtain:

$$L = 543\ \text{km}\quad W = 72\ \text{km} \tag{2}$$

For a magnitude $M = 8.8$ from formulas (1) it is obtained:

$$L = 817\ \text{km}\quad W = 90\ \text{km} \tag{3}$$

Thus, the estimate of the length L of the rupture in the source, the width of the rupture plane W gives values close to those in (Soloviev and Go, 1975; Diaz, 1992; Okada, 1992), (see Fig. 7b).

5. MATHEMATICAL FORMULATION OF THE PROBLEM

A system of nonlinear shallow water equations is used to describe the simulation of tsunami generation and propagation (Voltzinger et.al, 1989, Lobkovsky et.al, 2006; Lobkovsky et.al, 2017). The depth of the basin depends on both spatial coordinates and time, which allows account for the seabed displacement the during an earthquake. The equation of continuity describes the relationship between the displacement of the bottom and the water surface. In numerical simulation, a bathymetric map of the Pacific Ocean with a one-minute of isobath section was used, which includes the area of 4.000 - 47.6167 S, 65.9500 - 87.4667 W. Bathymetry contains 2618 × 1292 points. The simulation was performed with time step in 1 s. At a depth of 5 m, the condition of total reflection (vertical wall) is set, which makes it possible to fix the maximum and minimum values of the wave level displacement at this depth. The difference scheme from the book (Marchuk et al., 1983), which approximates shallow water equations (Voltzinger et.al, 1989) was taken as a basis. The scheme is based on spaced-apart template, which, in combination with the central-difference approximation of the spatial derivatives, simplifies the numerical implementation of the boundary conditions.

6. PRELIMINARY ANALYSIS OF THE DYNAMICS OF THE EARTHQUAKE SOURCE

For the numerical simulation of this earthquake process, the keyboard-block model was used (Lobkovsky and Baranov, 1984; Lobkovsky et al., 2017; 2021), which makes it possible to fragment the earthquake source into a number of keyboard blocks with further kinematic block motion. The displacement of each block in the earthquake source occurs by a different amount for a different time. When numerically simulating an earthquake and generating tsunami waves, the keyboard model of an earthquake source allows one to obtain a complex distribution of maximum wave heights on the coast, for a given dynamics of block movement in the earthquake source. The coordinates of the earthquake epicenter for given computation are taken from SHOA, 1997 (see Table 1).

6A - Scenario 1. Seismic source of 8 blocks

Initially, the authors considered scenarios with a rough fragmentation of the seismic source area into large blocks from 4 to 8. In this work, the first is the Scenario for an 8-block source from the general series of computations, designated here as Scenario 1.

Fig. 8 shows an 8-block source formed from available data, taking into account the distribution of the maximum tsunami wave heights along the coast, the phase of the first wave approach, and the number of waves approaching a given point (Soloviev and Go, 1975; Diaz, 1992; Gusiakov, 2021). Taking into account the available data, those movements in the source of the earthquake were selected that would be able to adequately simulate the processes on the coast. So in Chanabaya, Punta Lobos, Huanilios, the change in ocean level began with low tide. And in the points of Tocopilla, Cobija, Mejillones, the tsunami began with a rise in the water level. All these changes in levels were given in Table 4. The (+) sign corresponds to the upward displacement of the block in the seismic source; sign (-) corresponds to a downward shift (which corresponds to the wave run-up and rundown from the coast).

Table 4. Sequence of movement of blocks for Scenario 1.

Move ment	Block Lumber	1	2	3	4	5	6	7	8
	Height (m)	-4	5	4	-4	3	4	-3	4
1	Start time of movement (s)	30	0	70	50	110	90	165	130
	Final time of movement (s)	50	30	90	70	130	110	180	165

In this scenario, the trend of the blocks is a sequential movement from south to north. The first movements of keyboard blocks with the maximum amplitude are in the earthquake epicenter area.
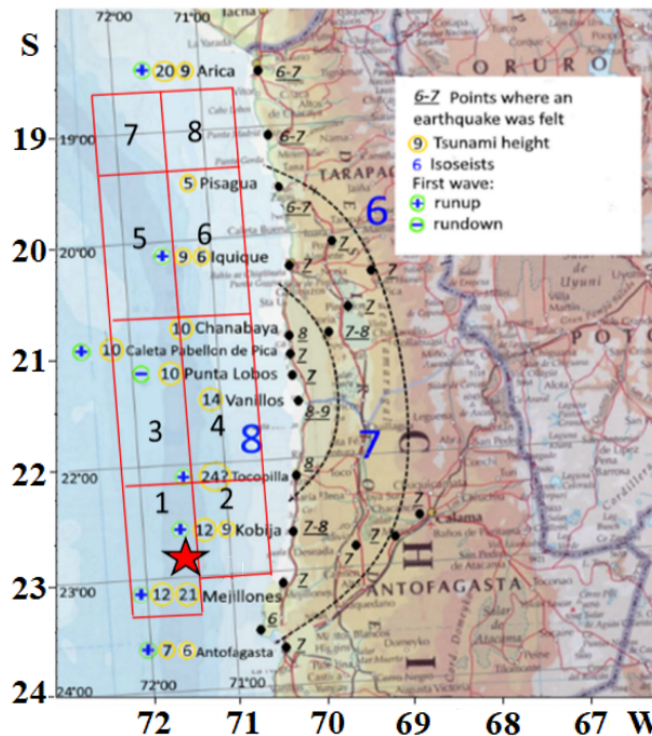

Fig. 8. Keyboard-block source of the Chilean earthquake of 1877 (Scenario 1). 8-block earthquake source, according to updated data (543 x 72 km). The red star indicates the earthquake epicenter.

Moreover, blocks numbered 1, 4 and 7 are moving down. The rest of the blocks move up sequentially (see Table 4). The first panel in the Fig.9 shows time moment during the generation of the tsunami source. In panel 2, the first wave front reaches the Chilean coast near Tocopilla and Cobija. Panels 3-5 show sequentially propagating wave fronts. Panel 6 shows the maximum wave height distribution over the water area when this scenario is
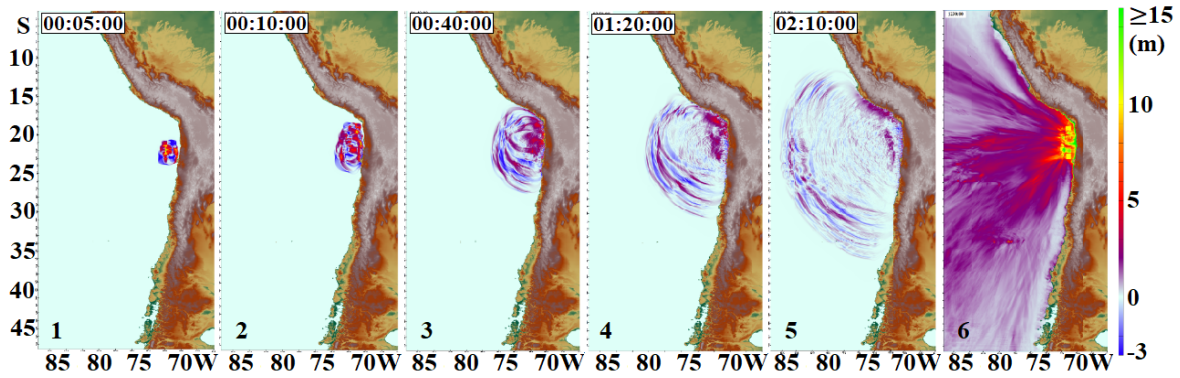
Fig. 9. Propagation of tsunami waves under scenario 1 (numbers 1–5) and distribution of maximum wave heights (6).

implemented. Wave heights on the coast are recorded at the 5-meter isobath. According to the results of this scenario, it can be seen that the average wave heights on the entire coast of the considered zone are not less than 15 meters, which is confirmed by the following histogram of the maximum wave height distribution along the coast (Fig. 10). It is clearly seen that the maximum wave heights on the coast reach 38 m, which is significantly different from the documentary data. Panels 1, 2 show a picture of the tsunami source generation. In panel 3, the first wave front reaches the coast of Chile between Antofagasta and Arica. Panels 3-7 show sequentially propagating wave fronts. Panel 8 shows the distribution of the maximum wave heights over the water area.
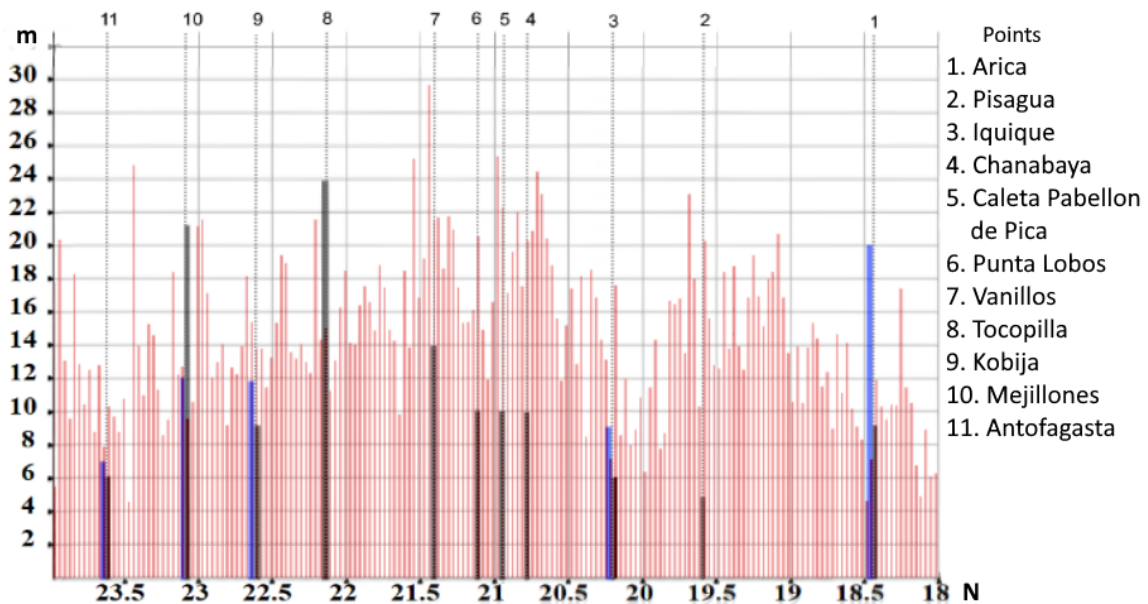

Fig. 10. Histogram of the distribution of the maximum heights of tsunami waves along the considered section of the coast for a 8-block source: red color – computed histogram; gray - data according to the catalogue by S. L. Soloviev and Ch.H.Go; blue - data from works (Diaz, 1992; Barrientos and Ward, 2009; Comte and Pardo, 1991). (Scenario 1).

Wave heights on the coast are recorded at the 5-meter isobath. According to the results of this scenario, it can be seen that the average wave heights on the entire coast of the considered zone are not less than 15 meters, which is confirmed by the following histogram of the distribution of the maximum wave heights along the coast (Fig. 10). It is clearly seen that the maximum wave heights on the coast reach 28m, which is significantly different from the documentary data. Based on the histogram for a visual comparison with documentary data, the following Table 5 can be constructed:

Table 5. Real and computed, according to Scenario 1, data on wave heights

Earthquake data											
No.	1	2	3	4	5	6	7	8	9	10	11
Point \ Data	Arica	Pisa-gua	Iqui-que	Chana-baya	Caleta Pabellon de Pica	Punta Lobos	Vani-llos	Toco-pilla	Co-bija	Mejil-lones	Anto-fagasta
Real data,m	9 (20)	5	6 (9)	10	10	10	14	24	9 (12)	21 (12)	6(7)
Scenario 1,m	7	20	7	19	22	20	22	15	14	12	10

As seen from the Table 5, at most points, the wave heights significantly exceeded the field data. Especially in the central cities (Chanabaya, Caleta Pabellon de Pica, Punta Lobos). It should be noted that in the column (Real data) for some items there are two numbers that are significantly different from each other. This is due, as noted above, with different documentary data presented in the works (Soloviev and Go, 1975; Diaz, 1992; Okada, 1992; Barrientos and Ward, 2009; Gusiakov, 2021).

6B Scenario 2: 12 - block earthquake source

Additional analysis of Scenario 1 made it possible to conduct a more accurate comparison of all available field data with the computed ones. Based on the results, in which the wave heights significantly exceeded the field data (excluding Mejillones and Tocopilla), the movement of the blocks was corrected. As a result, the subduction zone was segmented into a larger number of blocks, while leaving the source contour unchanged. So, in Fig. 11a you can see a newly formed source, consisting of 12 key-blocks, and the amplitudes of block movements have been also changed. In addition, the amplitudes of block movements were changed.

Since, in Chanabaya, Punta Lobos, Huanilios, the change in ocean level began with low tide, it was decided that blocks 6 and 8 closest to them were shifted down. It is analogical, since in the points of Tocopilla, Cobija, Mejillones the tsunami began with a rise in the water level, the movement of blocks 2 and 4 began with their moving up. Table 6 of block movements for Scenario 2 can be presented as follows
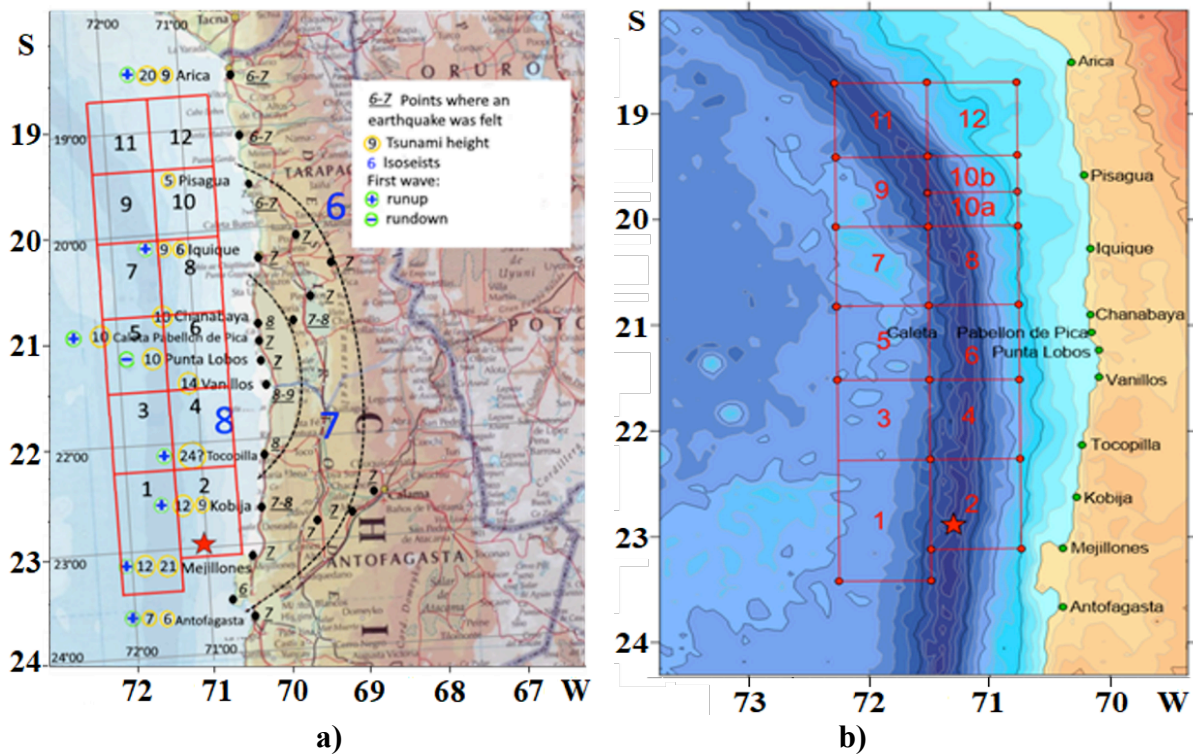
Fig. 11. The source of the earthquake of 1877: a) 12 blocks (Scenario 2); b) 13 blocks (Scenario 3).

Table 6. Block movements for Scenario 2

Move-ment	Block number	1	2	3	4	5	6	7	8	9	10	11	12
1	Height (m)	-3.5	3.5	10	8	2	-4	1.8	-1.8	1.5	-1	-3	5
	Start time of movement (s)	135	120	90	60	30	0	45	15	105	75	165	150
	Final time of movement (s)	150	135	105	75	45	15	60	30	120	90	180	165

On panels 1 and 2, it can be seen a complex wave front at the initial time moment. Then, the wave front takes on the usual circular shape. The wave reached the central part of the coast under consideration in 7-10 minutes (Chanabaya, Punta Lobos, Tocopilla, Cobija), in 15-20 minutes to the cities of Antofagasta, Mejiliones. Based on the computation results, the histogram of the distribution of the maximum wave heights is shown below (Fig. 13). As compared with computations on Scenario 1, in the area of the settlement of Iquique, the wave heights decreased. However, in the area of central settlements, they increased markedly, and began to exceed the field data significantly. Thus, the considered kinematics of movement of the keyboard blocks in the earthquake source and the displacement values of the blocks require further correction.
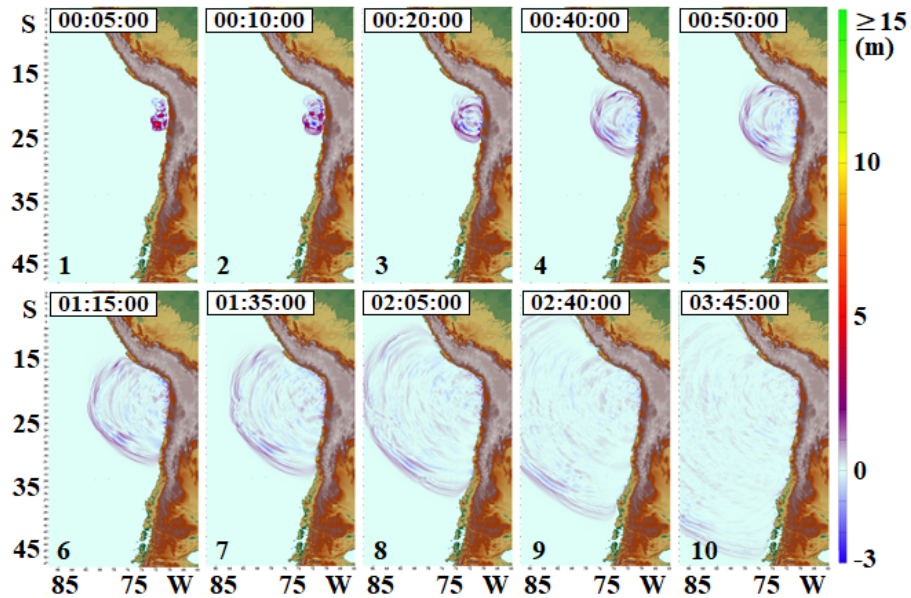
Fig. 12. Generation of the tsunami source and propagation of wave fronts for 10 times moments (Scenario 2).
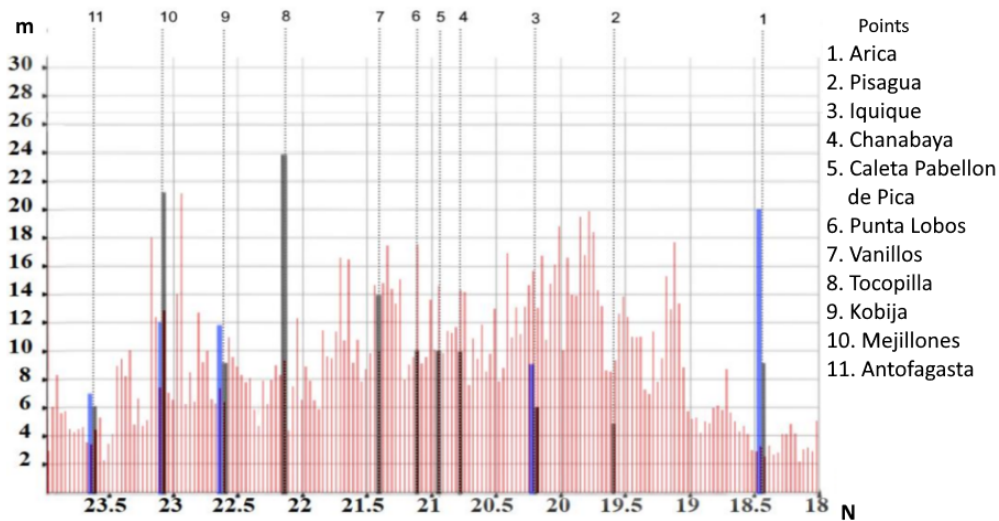

Fig. 13. Histogram of the distribution of the maximum heights of tsunami waves along the considered section of the coast for a 12-block source: red color – computed histogram; gray - data according to the catalog by S. L. Soloviev and Ch.N. Go; blue - data from works (Diaz, 1992; Barrientos and Ward, 2009; Comte and Pardo, 1991). (Scenario 2)

6C - Scenario 3: 13-block source

Based on the last two scenarios and taking into account the distribution of wave heights in the area of Iquique and Pisagua, the nearby block (block 10) was segmented to more small ones. Such segmentation of block 10 allows the movement of the seabed in the source to be corrected.
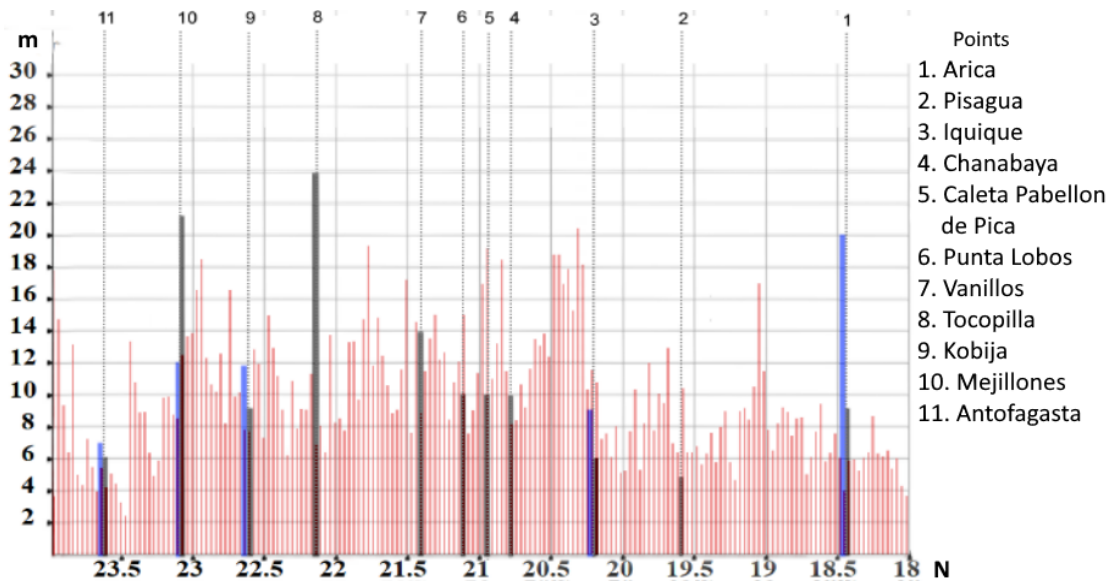
Fig. 14. Histogram of the distribution of the maximum heights of tsunami waves along the considered coastal area for a 13-block source: red color - calculated histogram; gray - data according to the catalogue by S. L. Soloviev and Ch.N Go; blue - data from works (Diaz, 1992; Barrientos and Ward, 2009; Comte and Pardo, 1991). (Scenario 3).

This helps to more accurately determine the wave height distribution in the settlements: Pisagua and Iquique. Thus formed 13-block earthquake source is shown in Fig. 11b. Based on the results of this computation, below is a histogram of the distribution of the maximum wave heights (Fig.14). The histograms of Scenarios 2 and 3 are similar, but there are a number of differences. In the area of Arica, an increase in the maximum wave heights is noticeable, which is associated with an increase in the vertical shift of movement of block 2. It can be seen that at the points of Punta Lobos, Calet-Pabellon de Pica, the wave heights approached the documentary data, but at the points, Pisagua and Iquique the values of the wave heights diverged significantly. Successive analysis of the computed results for Scenario 3 indicates a positive trend in the approach of waves to field data. However, at the points of Tocopilla, Cobija and Mejillones, significant differences in the results of computations and documentary data are visible. The histograms of Scenarios 2 and 3 are close to each other (see Fig. 13 and Fig. 14), however, there are a number of differences in the computations. In the area of Arika, an increase in the maximum wave heights is noticeable, which, apparently, is associated with an incorrect value of the displacement of block 2.

Since, as can be seen from the analysis of Scenarios 2,3, we have not yet achieved close coincidence with documentary data in a number of points. The goal of the next scenario is to achieve an approximation to the documentary data of waves at the points of Iquique and Pisagua, Tocopilla, Vanilios and Cobija, where the documentary data are much higher than the computed ones.

7. NUMERICAL SIMULATION WITH A CHANGED LOCALIZATION OF THE EARTHQUAKE SOURCE

Twelve computations were carried out with the available data on the localization of the source and epicenter of the earthquake. However, an additional analysis of the available data on the realization of this earthquake leads to the conclusion about the possible incorrect information on the localization of the epicenter of the earthquake on May 9, 1877. Taking into account such possibility the epicenter of this earthquake, under present numerical simulation, it was assumed to be shifted by about 21 ° latitude (Fig. 15). And the coordinates of the epicenter of the earthquake for further computations are proposed to be (21 S, 71.3 W). Changing the localization of the earthquake epicenter, a more complex seismic source was formed, comprising 14 blocks. Having analyzed the dynamics and direction of tsunami waves approaching the coast from the moment the earthquake began, the times of approach and the height of approaching waves on the coast, the direction of movement of blocks in the model seismic source was changed, corresponding to the direction of the rupture displacement in the earthquake source.

Thus, it was determined that the movement of blocks when modeling the dynamics of rupture in the source of the earthquake of 1877 should be directed from the earthquake epicenter (see Fig. 15) to the north-west and south-west alternately, taking into account the time of wave arrival to a specific point on the coast.
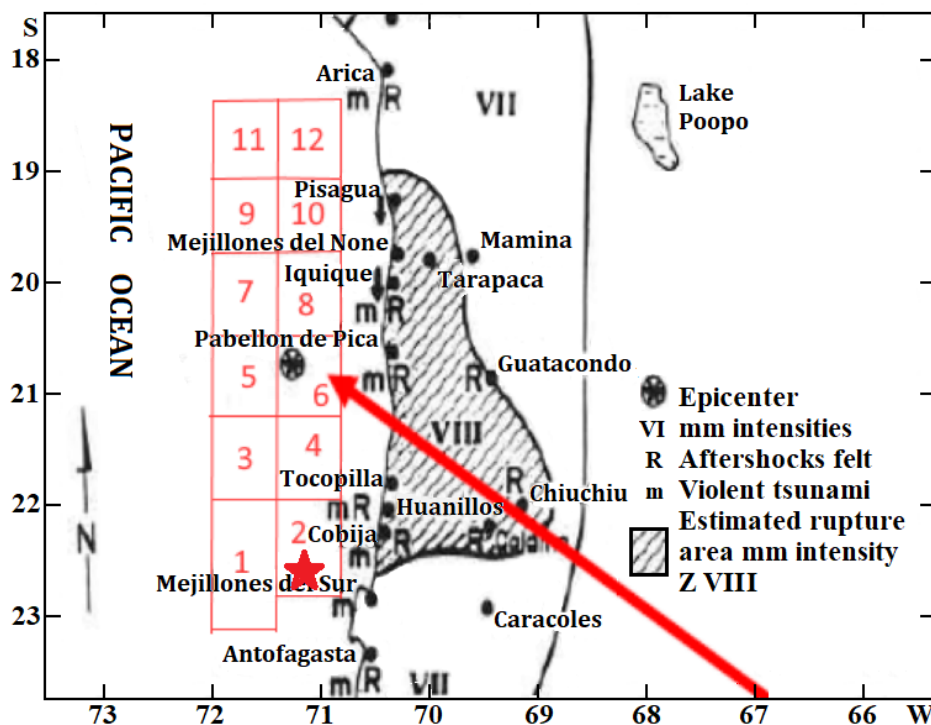

Fig. 15. Corrected epicenter of the 1877 earthquake Chile (block 6 (21 S, 71.3 W). (Kausel and Campos, 1992). Initial epicenter (block 2, red asterisk, 21.1 S, 71.3 W).

8. 14 - BLOCK SEISMIC SOURCE. SHIFTED EARTHQUAKE EPICENTER- (SCENARIO 4)

In Fig. 16 below, one can see a complex keyboard block source of the earthquake under consideration with an earthquake epicenter in the area of Caleta Pabellon de Pica. The block 4 being segmented into two sub-blocks allows the movement of the seabed in the source to be corrected. This allows one to more accurately select the distribution of waves in the settlements: Vanilios, Tocopilla and Cobija and others. In this scenario, blocks 4a and 4b will move sequentially and rise higher than in the previous ones. The location of blocks 4a and 4b has been adjusted to reflect the bottom topography near these points. When considering the area of settlements Chanabaya, Iquique, Pisagua, the analysis becomes more complex. An additional, third, offset of some blocks is introduced. With the new localization of the earthquake epicenter and the dynamics of the earthquake source, 11 additional scenarios of computations were carried out. Here, as more closer to some documentary data, scenario 4 (scenario 23) is given, where an additional, third offset is introduced for blocks 1, 4a, 7, 11 (see Table 7).
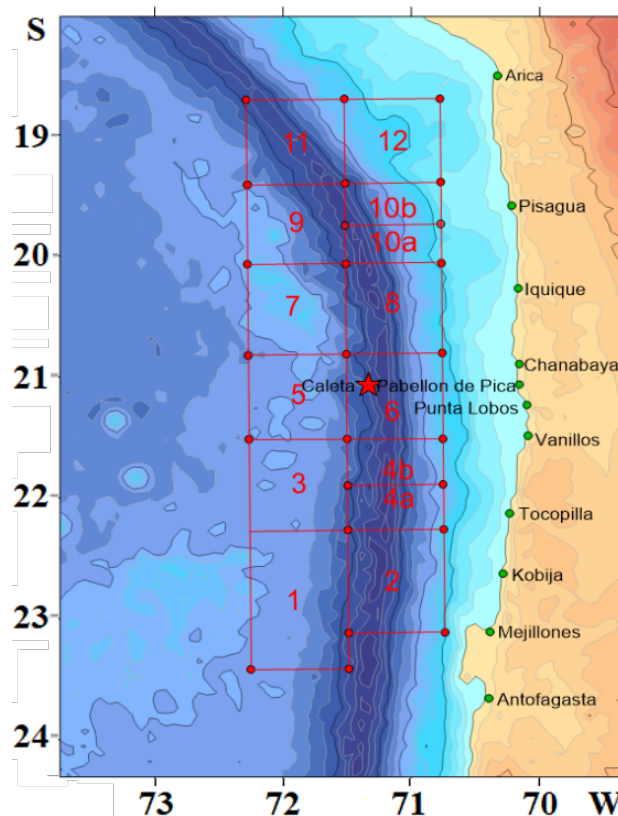

Fig. 16. Source of the earthquake of 1877: 14 blocks (Scenario 4)

Table 7. Sequence of movement of blocks for Scenario 4

Move ment	Block Lumber	1	2	3	4ᵃ	4b	5	6	7	8	9	10ᵃ	10b	11	12
1	Height (m)	-3,5	2	5,5	3,5	3	0	-3	1	-1	1	1,5	-3	2	4
	Start time of movement (s)	90	75	60	30	30		15	0	0	45	45	45	120	105
	Final time of movement (s)	105	90	75	45	45		30	15	15	60	60	60	135	120
2	Height (m)	3			1,5									1,5	
	Start time of movement (s)	165			150									135	
	Final time of movement (s)	180			165									150	

Figure 17 shows a histogram of the distribution of the maximum tsunami wave heights along the considered coastal area for a 14-block seismic source for Scenario 4.
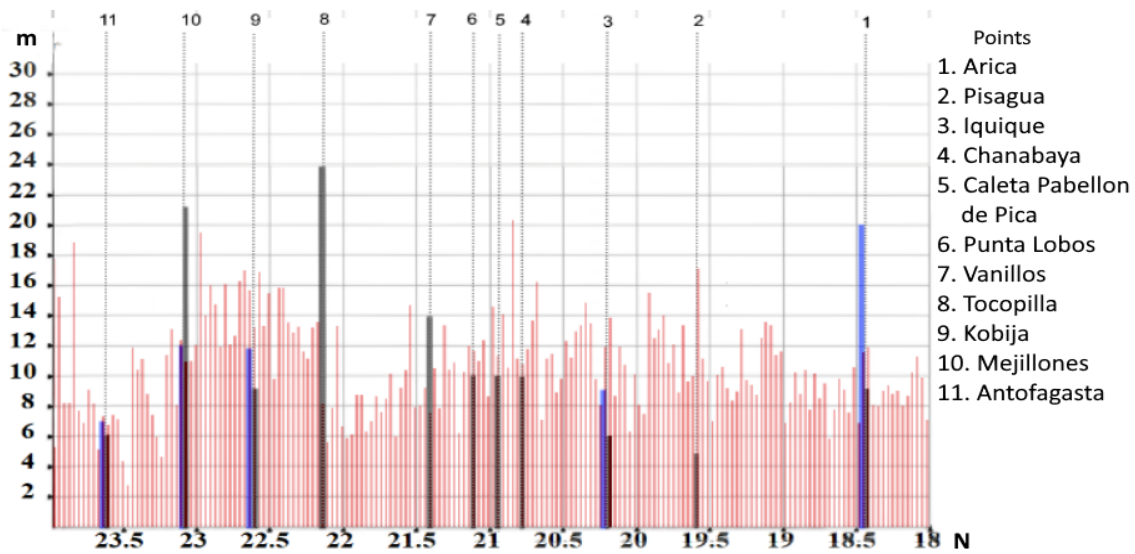

Fig. 17. Histogram of the distribution of the maximum heights of tsunami waves along the considered coastal area for a 14-block source: red color - calculated histogram; gray - data from the catalogue by S. L. Soloviev and Ch.N. Go; blue - data from works (Diaz, 1992; Barrientos, and Ward, 2009; Comte and Pardo, 1991). (Scenario 4).

Figure 18 shows the picture of the propagation of tsunami waves for 9 times moments and the distribution of the maximum wave heights over the computed water area. Panel 1 shows the generated tsunami source, and panels 2-9 show sequentially propagating wave fronts over the computed water area. Panel 10 shows the maximum wave heights distribution over the water area. Table 8 shows the computation data for the selected scenarios.

It can be seen that with an increase in the segmentation of the blocks from which the earthquake source was made into smaller ones (Scenarios: 1 → 2 → 3 → 4), the computation data noticeably approached the documentary data. When changing the localization of the earthquake epicenter and the appropriate selection of the kinematic movement of the keyboard blocks, the values of the wave heights most consistent with data were obtained (scenario 4).
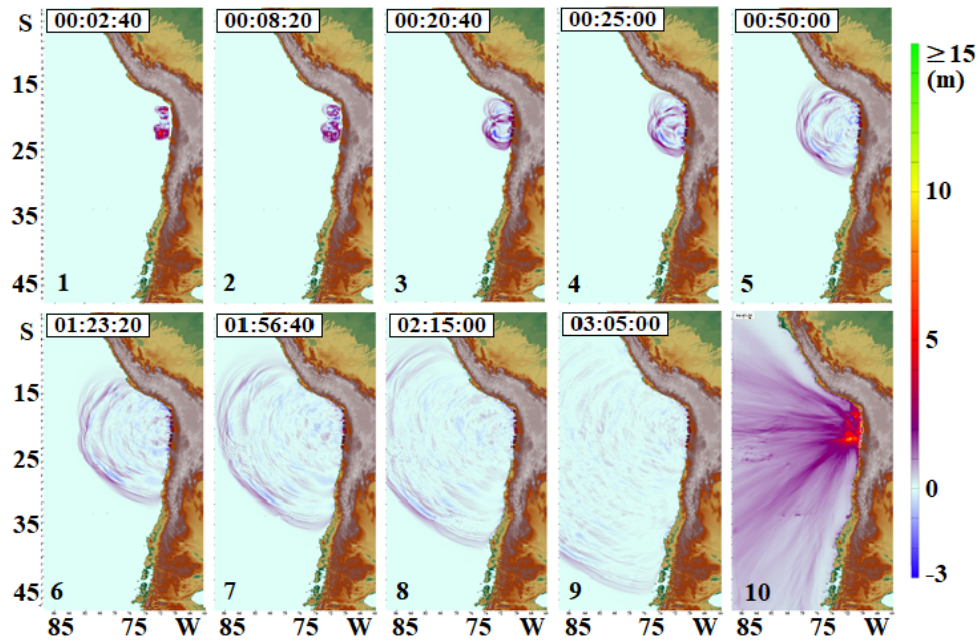

Fig. 18. Tsunami wave propagation under scenario 4 (numbers 1–9) and distribution of maximum wave heights in the computation water area (10)

Table 8. Results of numerical modeling of the seismic source and computations of the heights of tsunami waves with a changed localization of the epicenter of the 1877 earthquake

Points	Arica	Pisagua	Iquique	Chana-baya	Caleta Pabellon de Pica	Punta Lobos	Vanill os	Tocopill a	Kobija	Mejill ones	Antofag asta
Real data, m	9 (20)	5	6 (9)	10	10	10	14	24	9 (12)	21 (12)	6 (7)
Scenario 1	7	20	7	19	22	20	22	15	14	12	10
Scenario 2	3	9	15,5	14	14,5	17,5	10	9	6	8	4
Scenario 3	8	6	7	8	11	18	19	14	15	14	5
Scenario 4	7	12	13	8	8	12	11	11	12	10	12

The most adequate, seems to be the scenario 4 (scenario 23 from a series of computations). The computation was carried out on a 5-meter isobath, which allowed us to reduce the computation time for each scenario and choose the best one according to the given wave heights on a particular isobath. At the same time, the wave height on the shore will be different, namely, slightly higher, since when recalculating from isobath to shore for the considered points of this coast, the recalculation coefficients evaluated are in the range

from 1.07 to 1.8. (see, for example, (Pelinovsky & Mazova, 1992).

Thus, the performed analysis leads to positive results in the simulation of tsunami waves showed that the keyboard-block model of the subduction zone, even in a simplified kinematic formulation, most adequately describes the possible mechanism of the seismic process. You can see that the histogram has "outliers" in a number of points, which, in general, correspond to ambiguous documentary data on the event in question.

CONCLUSIONS

The article deals with a historical event: an earthquake and tsunami on May 9, 1877 with a source located off the northwestern coast of Chile. Within the framework of the keyboard-block model of the earthquake source, the article considers 4 series of calculations with different segmentation of the earthquake source. In total, 23 scenarios were considered, of which 4 calculations are presented in the article with the characteristics of the wave fields closest to each option along the Chilean coast. The transition from series to series is associated with increased segmentation, i.e. by changing the size of the blocks in the earthquake source, it made it possible to obtain closer values for the distribution of maximum wave heights along the coastal area of the central part of Chile. The choice of the dynamics of the seismic source was complicated by significantly different historical data, both on the recorded wave heights on the coast after the of tsunami waves propagation, and inaccurate data on the localization of the earthquake epicenter. The results of calculating the maximum wave heights for 4 various source segmentations show that the keyboard-block source model used in our work to model the generation and propagation of a tsunami wave for the Chilean coast seems to be the most suitable for the 1877 tsunami. The use of a simplified geodynamic model of the Lobkowski seismic source made it possible to obtain the most adequate model solution in terms of less discrepancy between model and historical data for a number of coastal areas.

ACKNOWLEDGEMENTS

REFERENCES

Abe, K., (1972). Tsunami and mechanism of great earthquakes. *Physics of the Earth and Planetary Interior*, *7,* 143-153.

Araneda, M., Avendaño, M.S., Díaz, Gerardo del Río, (2003). Cambios físicos detectados después del sismo de 1995, Antofagasta, Chile. Revista Geofísica Nº59. Instituto Panamericano de Geografia e Historia IPGH. https://www.revistasipgh.org/index.php/regeofi/article/view/565

Barrientos, S., Ward, S.N. (2009). The 1868 (Southern Peru) and 1877 (Northern Chile) tsunamis recorded at Fort Point, California. *XII Congreso Geológico Chileno Santiago*, 22-26 Noviembre, 2009.

Chlieh, M., Perfettini, H., Tavera, H., Avouac, J. P., Remy, D., Nocquet, J. M., Bonvalot, S. (2011). Interseismic coupling and seismic potential along the Central Andes subduction zone,. *Journal of Geophysical Research: Solid Earth,* 116, Vol. B12

CIGIDEN (2017) "Elaboración de un escenario sísmico en Iquique" pp.17-23 Santiago, Chile.

Comte, D., & Pardo, M. (1991). Reappraisal of Great Historical Earthquakes in the Northern Chile and Southern Peru Seismic Gaps, *Natural Hazards, 4,* 23-44.

DATA (2021) Materials of "Centro Ingeniería Mitigación Catástrofes Naturales Facultad de ingeniería (University of Antofagasta, Chile).

Diaz, J. (1992). Estudio de Fuentes de Tsunamis y de Terremotos: Aplicación en el Norte de Chile y Sur de Perú. Tesis para optar el título profesional de Oceanógrafo. Escuela de Ciencias del Mar, Facultad de Recursos naturales, Universidad Católica de Valparaíso

Electronic bathymetry Gebco Digital Atlas [Electronic resource]. - Access mode: http://www.gebco.net

González-Carrasco, J.F., González, G., Aranguiz, R., Melgar, D., Zamora, N., Shrivastava, M.N., Das, R., Catalan, P.A., Cienfuegos, R. (2020). A hybrid deterministic and stochastic approach for tsunami hazard assessment in Iquique, Chile. *Natural Hazards, 100,* 231–254.

Gusiakov, V.K. (2021), Global Tsunami Database, 2100 BC to Present, (2021). Novosibirsk Tsunami Laboratory, Institute of Computational Mathematics and Mathematical Geophysics, 4. Siberian Division of the Russian Academy of Sciences, Available at: https://tsun.sscc.ru/nh/ tsunami.php, Accessed 19.06.2021.

Iida K. (1963) A relation of earthquake energy to tsunami energy and the estimation of the vertical displacement in a tsunami source.- J.Earth Sci, Nagoya Univ., v.11, N.1, p.49-67.

Kanamori, H., & Stewart, G.S. (1978). Seismological aspects of the Guatemala Earthquake of February 4, 1976. *Journal of Geophysical Research: Solid Earth* 83(B7), 3427-3434.

Kausel, E. & Campos, J., (1992). The *M* = 8 tensional earthquake of 9 December 1950 of northern Chile and its relation to the seismic potential of the region. *Physics of the Earth and Planetapy Interior*, *72*, 220—235.

Kulikov, E.A., Rabinovich, A.B., & Thomson, R.E. (2005). Estimation of tsunami risk for the coasts of Peru and Northern Chile. *Natural Hazards*, *35*(2), 185-209; https://doi.org/10.1007/ s11069-004-4809-3

Lay, T., & Kanamori, H. (1981). An asperity model of large earthquake sequences. Earthquake prediction: An international review. Washington, D.C.: AGU. 1981. P. 579–592.

Lobkovsky, L. I., & Baranov, B.V. (1984). Keyboard model of strong earthquakes in island arcs and active continental margins. *Doklady of the Academy of Sciences of the USSR. 275*, 843-847 (in Russian).

Lobkovsky, L.I., Mazova, R.Kh., Kataeva, L.Yu., Baranov B.V. (2006). Generation and propagation of catastrophic tsunamis in the Sea of Okhotsk. Possible scenarios. *Doklady RAS. . 410*, 528-531.

Lobkovsky L.I., .Baranov G. B., Mazova R., Baranova N., 2017. Modeling Features of Both the Rupture Process and the Local Tsunami Wave Field from the 2011 Tohoku Earthquake // Pure Appl. Geophys. (2017). V.174, p. 3919-3938, doi:10.1007/s00024-017-1539-5 (March 2017) pp.1-20.

Marchuk, A.G., Chubarov, L.B., Shokin, Yu.I. (1983). *Numerical modeling of tsunami waves*. (Nauka Press, Moscow, USSR, in Russian).

Mazova, R.Kh., & Ramirez, J.F. (1999). Tsunami waves with an initial negative wave on the Chilean coast. *Natural Hazards 20*, 83-92.

Mazova R.Kh., Tyuntyayev S., Giniyatullin A. EtAl., 2020. Numerical Simulation of Earthquakes and Tsunami in Mexico. Case Study: Earthquake and Tsunami of 8 September 2018//STH, V.39, N 4, p.210-227 (2020).

Mendoza, C., (1997). (USGS) "Basic Seismology for Geotechnics, Construction and Risks", course. Faculty of Engineering. University of Antofagasta. 6-7 Nov 1997. (private communication).

Okada, Y. (1992). Internal deformation due to shear and tensile faults in a half-space. *Bulletin of Seismological Society of America 82*, 1018-1040.

Okal, E.A., Borrero, J.C., Synolakis, C.E. (2006). Evaluation of tsunami risk from regional earthquakes at Pisco, Peru. *Bulletin of Seismological Society of America 96*, 1634–1648. https://doi.org/10.1785/ 0120050158

Pararas-Carayannis, G. (2010). The earthquake and tsunami of 27 February 2010 in Chile - Evaluation of source mechanism and of near- and far-field tsunami effects. *Science of Tsunami Hazards 29*, 96-126.

Pelinovsky, E. (1996). Hydrodynamics of tsunami waves. (IAP of the Russian Academy of Sciences, Nizhny Novgorod, RUSSIA).

Ramirez, J. Titichoca, H. Lander, J. & Whiteside, L. (1997). The minor destructive tsunami occurring near Antofagsta, northen Chile, July 30 1995. *Science of Tsunami Hazards*, *15*(1), 3-22.

Riquelme, S., Schwarze H., Fuentes M., & Campos J. (2020). Nearfield effects of earthquake rupture velocity into tsunami runup heights, *Journal of Geophysical Research*. *125*(6), e2019JB018946.

Ruiz, S, & Madariaga, R. (2018). Historical and recent large megathrust earthquakes in Chile. *Tectonophysics 733*, 37-56, https:doi.org/10.1016/j.tecto.2018.01.015.

Ruiz, J.A., Fuentes, M, Riquelme, S., Campos. J., Cisternas. A. (2015). Numerical simulation of tsunami runup in northern Chile based on non-uniform k22 slip distributions. *Natural Hazards 79*, 1177–1198.

Silgado, E. (1985), Destructive Earthquakes of South America 1530–1894, Earthquake Mitigation Program in the Andean Region, Vol. 10, CERESIS, Lima, Peru, 328 pp.

Soloviev, S.L., and Go, Ch. N. (1975), Catalogue of Tsunamis on the Eastern Shore of the Pacific Ocean, Nauka, Moscow, 310 pp. [in Russian; English Translation: Canadian Transl. Fish. Aquatic Sci., No. 5077, Ottawa, 1984, 439 pp.].

Titichoca, H. & Guiñez, D. (1992). Recontitución paleogeográfica de las curvas de inundación producidas por tsunami en el norte de Chile Iquique-Arica en los años 1868-1877. II Congreso de Ciencias de la Tierra. Instituto Geográfico Militar Santiago Chile.

Vargas, G., Ortlieb, L., Chapron, E., Valdés, J., Marquardt C. (2005). "Paleoseismic inferences from high resolution marine sedimentary record in northern Chile (23°S)". *Tectonophysics 399* (1-4), 381-398.

Vidal Gormáz, F., "Datos sobre el terremoto del 9 de mayo de 1877" (1884) pp 193-221 Observatorio Astronómico. Imprenta Nacional. Santiago. Chile.

Wells, D.L., & Coppersmith, K.J. (1994) New empirical relationships among magnitude, rupture length, rupture width, rupture area, and surface displacement Bulletin of Seismical Society of America. *4,* 974-1002.

Voltzinger, N.E., Klevanny, K.A., & Pelinovsky, E.N. (1989). *Long-wave dynamics of the coastal zone,* (Gidrometeoizdat Press, Leningrad, USSR) (in Russian).

Tsunamis in Peru-Chile (noaa.gov).

NGDC/WDS Global Historical Tsunami Database (https://www.ngdc.noaa.gov/hazard/tsu_db.html).

Gebco Digital Atlas

SHOA, 1997